Characterisation and optimisation of a failure model for high strength aluminium alloys using Nakajima experiments

Schlosser, Julian; Mouchtar, Serkan; Schneider, Robert; Schanz, Jochen; Rimkus, Wolfgang; Harrison, David; MacDonald, Martin; Kulatunga, Muditha

Published in:
Advances in Manufacturing Technology XXXII

DOI:
10.3233/978-1-61499-902-7-399

Publication date:
2018

Document Version
Author accepted manuscript

Characterisation and optimisation of a failure-model for high strength aluminium alloys

Julian Marc Schlosser [ab], Serkan Mouchtar [a], Robert Schneider [a], Jochen Schanz [ab]
Wolfgang Rimkus [a], David K. Harrison [b], Martin Macdonald [b], Muditha Kulatunga [b]
[a]Lightweight Construction Centre, Aalen University, Beethovenstraße 1, 73430 Aalen, Germany.
[b]Department of Engineering and Built Environment, Glasgow Caledonian University, Cowcaddens Road, Glasgow, United Kingdom.

Abstract. In the present work an effective parameter identification for the evaluation of a failure model for FE-simulations has been carried out. This failure model is suitable to calculate different fracture elongation values among occurring triaxiality of a high-strength aluminium sheet metal alloy (AA7075). Various specimen geometries have been selected to achieve different loading states (triaxiality). For biaxial strains a forming limit curve (*FLC*) is converted by using mathematical formulations. To measure the equivalent local strains in the event of fracture an optical measurement system has been installed and adapted to a tensile testing machine. The failure curve and the material model which includes the extrapolated flow curve are implemented into the FE-simulation model. In order to improve the accuracy of the failure-curve a parameter optimization has been carried out. It shows that by using the optimised failure curve a high correlation between experimental and calculated force-displacement curves for any given specimen geometry can be achieved.

Keywords. Failure model, FEM, FEA, FLC, lightweight design, high strength aluminium alloys, AA7075

1. Introduction

Due to more stringent legislation for CO_2 emissions and because of energy scarcity the automobile manufacturers are faced with new challenges. In order to build more environmentally friendly cars one must focus on designing lightweight constructions where the amount of material (mass) and costs are decreased respectively [1]. This design philosophy requires exact knowledge of loads, boundary conditions, and, in the event of a crash, the failure behaviour of corresponding structural material. Lightweight construction materials, which have already been used in the aerospace industry for a long time and which are gradually being established in the automotive industry, are ultra-high strength aluminium alloys such as the AA7075 for example [2, 3]. In order to predict the material behaviour from the manufacturing process up to the event of a crash the whole material “history” need to be taken into account. While forming limit curves (FLC) are sufficient for forming simulations, however, they rather seem unsuitable for crash simulations due to co-occurring multiaxial loads. Thus, an accurate

damage model is crucial for a robust numerical prediction of the crash behaviour of e.g. AA7075 component. In this study the fundamentals of the TAB1 damage model in RADIOSS are given to get an overview of the theory behind the damage model. Subsequently, material parameters and the mechanical behaviour of EN AW-7075 in T6 state are listed and fitted into a material card using the v. Mises flow rule hypothesis. Further, to identify the fracture strain with optical measurement systems under various triaxiality states different tensile tests are carried out using various specimen geometries. Based on this experimental data a Triaxiality-Failure-Curve (*TFC*) is determined and calibrated with parameter optimisation to get optimised input parameters for the failure model.

2. Description of the failure model *fail_tab1*

The failure model *fail_tab1* in RADIOSS (similar as GISSMO in LS-DYNA) describes a strain failure model based on path-dependent damage accumulation using user-defined functions. This model is a phenomenological formulation of ductile damage and has established features of failure specifications, such as e.g. diffuse necking [4].
The usual notation is a characterization of various load states. In crash-simulations it is common practice that occurring stress is usually represented by the stress triaxiality η [5, 6]:

$$\eta = \frac{\sigma_m}{\sigma_{vm}} \tag{1}$$

In sheet metal forming it is a common assumption to use the plane stress case ($\sigma_3 = 0$). Consequently, the hydrostatic stress σ_m and the von Mises stress σ_{vm} are:

$$\sigma_m = \frac{\sigma_1+\sigma_2}{3} \tag{2}$$

$$\sigma_{vm} = \sqrt{\sigma_1^2 + \sigma_2^2 - \sigma_1 * \sigma_2} \tag{3}$$

The *fail_tab1* in RADIOSS calculates in increments, it is path dependent and gives different final results for different strain paths. The damage accumulation rule is given by:

$$\Delta D = \frac{\Delta\varepsilon_p}{\varepsilon_f} * n * D^{\left(1-\frac{1}{n}\right)} \tag{4}$$

Eq. (4) is evaluated and accumulated at every time step using the current value of damage (D), plastic strain increment ($\Delta\varepsilon_p$) and the equivalent fracture strain ($\varepsilon_f(\eta)$) as function of the triaxiality. A crack or element rupture occurs, if the damage parameter D is reached one. The failure strain is obtained by different tensile test geometries to reach various triaxiality and can be implemented into the simulation program by a Triaxial-Failure-Curve (*TFC*). An example can be seen in Figure 2.

3. Experimental

3.1. Material and mechanical behaviour

For this study an aluminium alloy with the designation EN AW-7075 in T6 state was used. Table 1 illustrates the composition specification of tested aluminium alloy.

Table 1. Chemical composition of AA7075 T6 (wt.-%)

Si	Fe	Cu	Mn	Mg	Cr	Ni	Zn	Ti
0.05	0.12	1.53	0.01	2.65	0.18	0.01	5.86	0.05

The tensile test is standardized according to DIN EN ISO 6892 [7] and is for the purpose of evaluating the mechanical behaviour of metallic materials subjected to a uniaxial tensile force. The aluminium flow curves (see Table 2), which are used for the *FEM* simulation, are extrapolated to a forming limit of $\varepsilon = 1$ using Hollomon`s law [8] (see Eq. (5)). Beyond the point of uniform elongation the flow curve is fitted iteratively by applying the least square method.

$$\sigma_f = C * \varepsilon^n \tag{5}$$

$$C = UTS * \left(\frac{e}{n}\right)^2 \tag{6}$$

where

$\sigma_f = yield\ stress$

$n = hardening\ parameter$

Table 2. Mechanical behavior of AA7075 T6

σ_f [MPa]	UTS [MPa]	e_{20} [%]	Flow curve
487	548	17	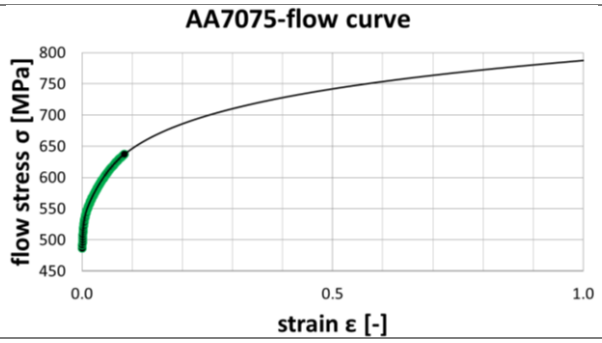

3.2. Optical measuring system and used specimen geometries for various load states

The optical measuring system, which is illustrated in Figure 1, was adapted to the tensile testing machine to measure local strains. In order to be able to measure the local strain a stochastic pattern is applied onto the surface of the specimens. Using this pattern the software "GOM Correlate" was used to calculate the distortions.

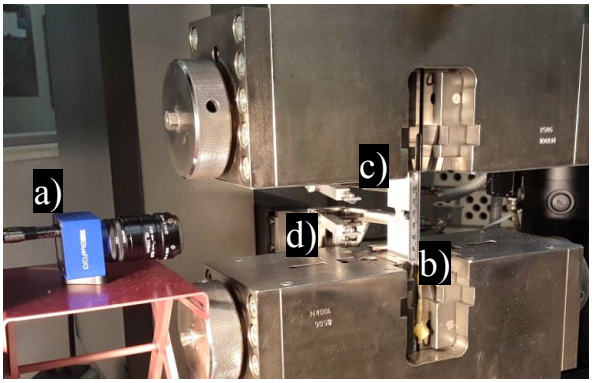

a) 1.3 Megapixel Camera
- photo size 1280x1024
- 5 frames per second
- monochrome camera

b) Scale for image calibration

c) Specimens and clamping device

d) Tactile extensometer
- For monitoring the force-displacement diagram

Figure 1. Test setup for local strain measurement

To achieve triaxiality-dependent failure strains specimens with different geometries are needed. Table 3 indicates all geometry variations used and corresponding results (ε_{eq} and η) reached in the experiment. With these specimens, the *TFC* can be defined in the range of $0 < \eta < 0.5$.

Table 3. Various shaped specimens to achieve different triaxiality

	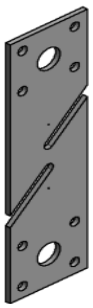		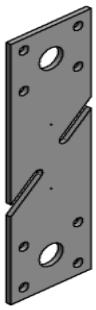					
specimens	Shear 0°		Shear 15°		Tensile		Notched	
Test results	ε_{eq}.	η	ε_{eq}.	η	ε_{eq}.	η	ε_{eq}.	η
	0.287	0.089	0.277	0.240	0.377	0.384	0.253	0.496

For all analysis the v. Mises yield function and associated flow rule, considering isotropic hardening, are used (M36_Plas_TAB RADIOSS & MAT_024 LS-DYNA). In order to be able to define the failure curve in the biaxial area an experimental test (biaxial state of the specimen) is usually needed. Thus, an existing Forming Limit Curve (*FLC*) of the AA7075 material [3, 9] used and respective value converted using following equations:

$$plane\ stress: \sigma_3 = 0 \tag{7}$$

$$small\ elastic\ deformations: \varepsilon_1 \approx \varepsilon_{p1}\ \&\ \varepsilon_2 \approx \varepsilon_{p2} \tag{8}$$

$$isotropic\ plasticity: \varepsilon_3 \approx \varepsilon_{p3} = -\varepsilon_{p1} - \varepsilon_{p2} \tag{9}$$

$$proportional\ loading: a = \frac{\varepsilon_2}{\varepsilon_1} \tag{10}$$

$$equivalent\ plastic\ strain: \varepsilon_{eq} = \frac{2}{\sqrt{3}} * \varepsilon_{p1} * \sqrt{1 + a + a^2} \tag{11}$$

$$triaxiality\ \eta = \frac{\sigma_m}{\sigma_{eq}} = \frac{1+\alpha}{\sqrt{3}*\sqrt{1+\alpha+\alpha^2}} \tag{12}$$

Table 4. Forming-limit diagram AA7075 [3, 9]

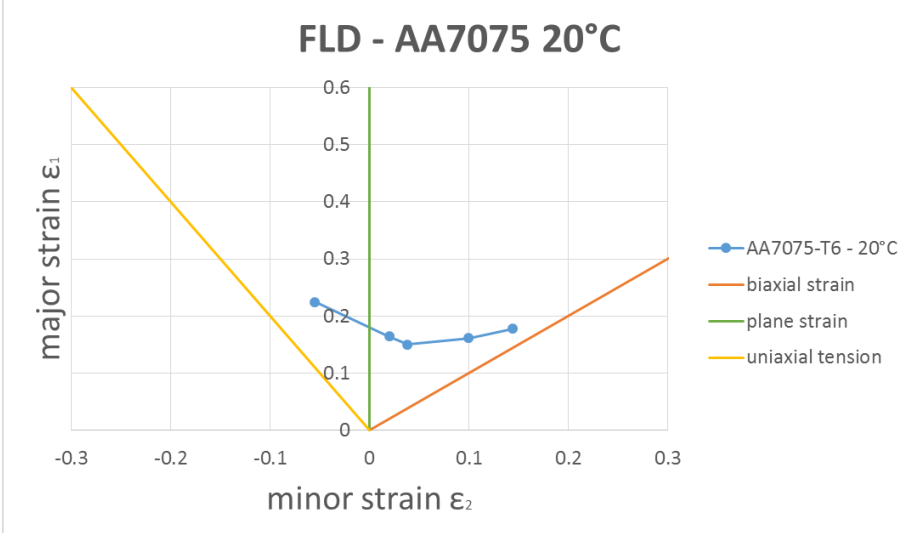

FLD converted by Eqs. (11) and (12)	
$\varepsilon_{eq}.$	η
0.202	0.607
0.199	0.630
0.263	0.661

0.322	0.665

4. Numerical calibration of the failure-curve using parameter optimisation

Figure 2 shows the results of the optical measurement and the values of the converted *FLD* (blue line) with individual standard deviations. The values of the standard deviations were also used as a restriction for parameter optimisation (upper and lower limit). The orange line in Figure 2 indicates the optimised failure curve within the pre-defined limits which can further be taken for any prediction of the force-displacement characteristic of the experiments (Figure 3).

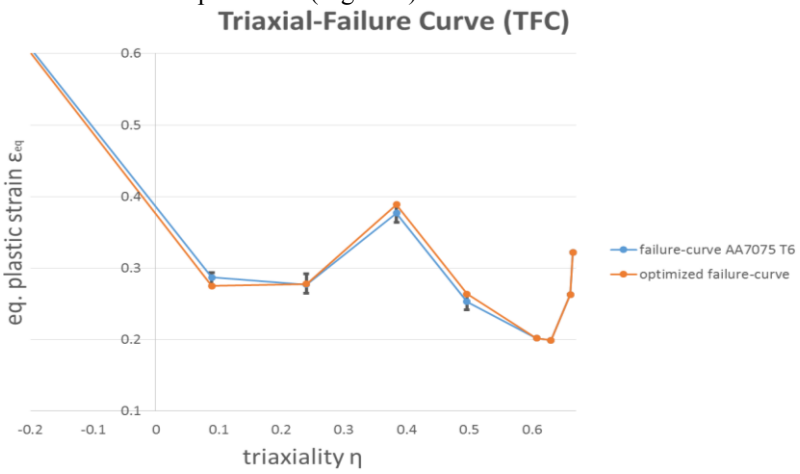

Figure 2. Triaxial-Failure Curve AA7075 T6

As optimization basis, the experimental force-displacement curves were taken into account. During the optimization process the equivalent plastic strain of each point (tensile-, shear 0°-, shear 15°- and notched test) is varied among the lower and upper limits in order to achieve the best fit between the experimental and simulated force-displacement curve. Figure 3 indicates the experimental force displacement curve (blue) which is compared with the initial *TFC* (blue curve in Figure 2) and the optimised *TFC* (orange) curve in Figure 2). It is shown that the optimised *TFC`s* are in good agreement with the experimental results.

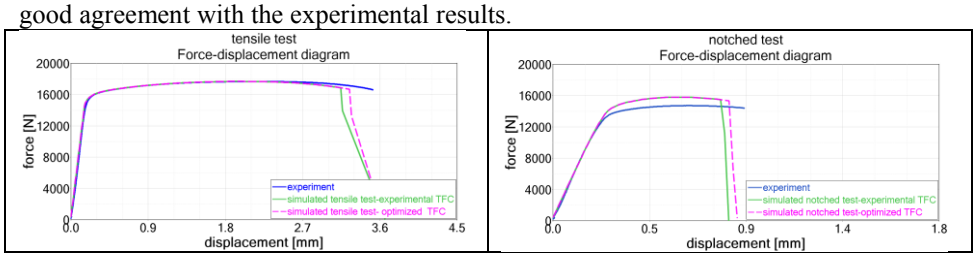

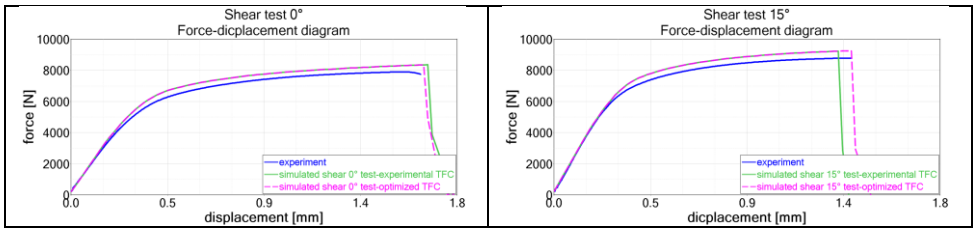

Figure 3. Force-displacement diagram; experiment-blue, average measurement values-green, optimized-purple

5. Conclusion

Experimental tests with various specimen geometries were carried out to determine the force-displacement characteristics of AA7075-T6 material. The local strains at fracture have been monitored under different stress conditions ($-1/3 < \eta < 2/3$) using an adapted optical measurement system. Respective values for $\eta = 2/3$ were taken from a forming limit diagram and converted. For the analysis the v. Mises yield function was considered and for the description of the materials hardening behaviour Hollomon`s law was used. Subsequently, a failure curve was optimised and fitted to experimental data using parameter optimisation methods. The predicted force-displacement data show good correlation with experimental results for all loading states (compression, shear, tensile and biaxial).

References

[1] McKinsey & Company, CO2-Regulierung sorgt bis 2030 für dreistelliges Milliardenwachstum im Leichtbau.
[2] J. Schlosser, R. Schneider, W. Rimkus, R. Kelsch, F. Gerstner, D.K. Harrison, R.J. Grant, Materials and simulation modelling of a crash-beam performance – a comparison study showing the potential for weight saving using warm-formed ultra-high strength aluminium alloys, J. Phys.: Conf. Ser. 896 (2017) 12091.
[3] Torsten Grohmann, Forming of AMAG 7xxx Series Aluminium Sheet Alloys (2016).
[4] Altair Engineering, RADIOSS Help: failure model tab1.
[5] J. Effelsberg, A. Haufe, M. Feucht, F. Neukamm, P. Du Bois, On parameter identification for GISSMO damage model.
[6] Daniel Hörling, Parameter identification of GISSMO damage model for DOCOL 1200M: A study on crash simulation for high strength steel sheet components, 2015.
[7] DIN EN ISO 6892-1, Zugversuch - Metallische Werkstoffe - Prüfverfahren bei Raumtemperatur, Beuth Verlag GmbH.
[8] J. H. Hollomon, Tensile deformation, Trans. Metall. Soc., 1945, pp. 268–290.
[9] AMAG, Hochfeste Aluminiumbleche der den Automobil-Leichtbau, Alu Report Automobil (2012) 6-9.